blood®
Regular Article

Check for updates

LYMPHOID NEOPLASIA

CDK7 controls E2F- and MYC-driven proliferative and metabolic vulnerabilities in multiple myeloma

Yao Yao,[1,2] Jessica Fong Ng,[1] Woojun Daniel Park,[3] Mehmet Samur,[1] Eugenio Morelli,[1] Jessica Encinas Mayoral,[4] Zuzana Chyra,[1] Yan Xu,[1] Sanika Derebail,[1] Charles Epstein,[5] Behnam Nabet,[6] Marta Chesi,[7] Nathanael S. Gray,[8] Richard A. Young,[9] Nicholas Kwiatkowski,[10] Constantine Mitsiades,[11] Kenneth C. Anderson,[1] Charles Y. Lin,[12] Nikhil C. Munshi,[1,13] and Mariateresa Fulciniti[1]

[1]Jerome Lipper Multiple Myeloma Disease Center, Dana-Farber Cancer Institute, Harvard Medical School, Boston, MA; [2]Blood Disease Institute, Key Laboratory of Bone Marrow Stem Cell, Xuzhou Medical University, Xuzhou, China; [3]Department of Molecular and Human Genetics, Baylor College of Medicine, Houston, TX; [4]University Hospital October 12, Madrid, Spain; [5]Broad Institute, Cambridge, MA; [6]Human Biology Division, Fred Hutchinson Cancer Center, Seattle, WA; [7]Comprehensive Cancer Center, Mayo Clinic, Scottsdale, AZ; [8]Department of Chemical and Systems Biology, Chem-H and Stanford Cancer Institute, Stanford Medical School, Stanford, CA; [9]Whitehead Institute for Biomedical Research, Cambridge, MA; [10]Kymera Therapeutics, Watertown, MA; [11]Department of Medical Oncology, Dana-Farber Cancer Institute, Boston, MA; [12]Kronos Bio, Cambridge, MA; and [13]VA Boston Healthcare System, Boston, MA

KEY POINTS

- **CDK7 acts as a central hub for the perturbed cyclin-dependent kinase-pRb-E2F pathway in MM cells.**
- **CDK7 inhibition impairs expression of key components of the MYC-dependent glycolytic cascade and aerobic glycolysis in MM cells.**

Therapeutic targeting of CDK7 has proven beneficial in preclinical studies, yet the off-target effects of currently available CDK7 inhibitors make it difficult to pinpoint the exact mechanisms behind MM cell death mediated by CDK7 inhibition. Here, we show that CDK7 expression positively correlates with E2F and MYC transcriptional programs in cells from patients with multiple myeloma (MM); its selective targeting counteracts E2F activity via perturbation of the cyclin-dependent kinases/Rb axis and impairs MYC-regulated metabolic gene signatures translating into defects in glycolysis and reduced levels of lactate production in MM cells. CDK7 inhibition using the covalent small-molecule inhibitor YKL-5-124 elicits a strong therapeutic response with minimal effects on normal cells, and causes in vivo tumor regression, increasing survival in several mouse models of MM including a genetically engineered mouse model of MYC-dependent MM. Through its role as a critical cofactor and regulator of MYC and E2F activity, CDK7 is therefore a master regulator of oncogenic cellular programs supporting MM growth and survival, and a valuable therapeutic target providing rationale for development of YKL-5-124 for clinical use.

Introduction

Cyclin-dependent kinases (CDKs) are a family of serine/threonine protein kinases that, together with their associated regulatory cyclins, control key aspects of the cell cycle and transcription. Human tumors frequently have dysregulated CDK-dependent cell-cycle control mechanisms,[1] making these mechanisms an attractive therapeutic target. Recurrent dysregulation of CDK activity has also been reported in multiple myeloma (MM), a plasma cell malignancy; however, therapeutic translation of cell cycle CDK inhibitors, including United States Food and Drug Administration–approved CDK4/6 inhibitors, has been hindered by a lack of single-agent efficacy, suggesting that targeting cell cycle regulation alone is insufficient to produce a durable response in MM.[2]

Among CDKs, CDK7 and its partners cyclin H and MAT1 uniquely sit at the intersection of cell cycle and transcriptional control. The trimeric complex acts as a CDK-activating kinase controlling other CDKs via phosphorylation of the T-loop, a key regulatory step required for CDK activity. Moreover, CDK7 is a component of the general transcription factor TFIIH, and it phosphorylates the C-terminal domain of the RNA polymerase II large subunit Rpb1,[3,4] helping to drive transcription initiation.

An aberrant increase in CDK7 levels has been detected in many different cancer types, and it often correlates with aggressiveness and poor prognosis. THZ1, an inhibitor of CDK7 as well as CDK12/13, blocks the growth of several cancer types including triple-negative breast cancer, non–small cell lung carcinoma and MYCN-driven neuroblastoma, suggesting that CDK7 inhibition might be an interesting therapeutic strategy for transcription-addicted cancers, including MM.[5-8] However, the fact that THZ1 also equipotently targets CDK12 and CDK13 has complicated a clear attribution of cellular phenotypes to CDK7 inhibition and has fueled efforts to develop more selective CDK7 inhibitors. Several other CDK7 inhibitors with varying degrees of selectivity have now been reported, 4 of which (ICEC0942, SY-1365, SY-5609, and LY340515) have progressed to phase 1/2 clinical trials.

Downloaded from http://ashpublications.net/blood/article-pdf/141/23/2841/2055728/blood_bld-2022-018885-main.pdf by guest on 06 May 2024

Here, we confirmed the functional consequences of CDK7 inhibition in MM using chemical and genetic approaches, including engineered systems for rapid CDK7 protein degradation (small molecule–coupled degron epitope [dTAG])[9]; and explored the efficacy of a recently reported highly selective CDK7 covalent inhibitor, YKL-5-124, which covalently targets a unique cysteine (Cys) residue (C312) located outside of the CDK7 kinase domain,[10] in relevant translational models of MM. YKL-5-124. We report that selective perturbation of CDK7 expression and activity disrupts MYC- and E2F-driven molecular programs in MM cells, while having little observable impact on normal cells. Moreover, by ultimately regulating MYC at the cellular level, CDK7 inhibition downregulates the expression of key glycolytic genes, impairing aerobic glycolysis and highlighting a central role for CDK7 in MM metabolic reprogramming. Given the dependence of MM on glycolysis for energy, these data provide rationale for therapeutic targeting of CDK7 in myeloma.

Material and methods

Cells

All myeloma cell lines were cultured in RPMI-1640 (Gibco) supplemented with 10% fetal bovine serum (Gibco, Life Technologies, Carlsbad, CA), 1% penicillin/streptomycin and 1% L-glutamine. Primary MM cells and bone marrow mononuclear cells were isolated from bone marrow aspirates of patients with MM after informed consent and institutional review board (Dana Farber Cancer Institute) approval. Peripheral blood mononuclear cells were isolated from fresh buffy coats from healthy donors and activated with 20 μg/mL phytohemagglutinin (InvivoGen, #inh-phap).

Chemicals

YKL-5-124 and dTAG^V-1 were kind gifts from N.S.G. Doxycycline was purchased from Sigma. Compounds were dissolved in dimethyl sulfoxide unless otherwise stated. Galactose was purchased from Sigma (G0750, Burlington, MA).

EMSA

Nuclear extracts were extracted from MM cells treated with 250 nM YKL-5-124 for 24 hours using the Nuclear Extraction kit (Signosis, #SK-0001). Nuclear extract (5 μg) was used in the E2F1 electrophoretic mobility shift assay (EMSA) (Signosis, #GS-0011), per the user manual.

E2F reporter experiment

H929 cells were infected with E2F1 reporter luciferase plasmid. E2F1 reporter activity was assessed using the Promega Luciferase reporter assay system.

Chromatin immunoprecipitation

MM cells (3×10^7) were treated with YKL-5-124 or dimethyl sulfoxide. Chromatin immunoprecipitation assay was performed in accordance with the manufacturer's instructions (Simple Chip Enzymatic Chromatin IP Kit, CST#9003) with the following antibodies: E2F1, immunoglobulin G (Millipore, #17-10061), and MYC (CST #13987). Primer sequences are in the supplemental Table1, available on the *Blood* website.

Statistical analysis

The significance of differences between experimental variables was analyzed using an unpaired Student *t* test, or analysis of variance for multiple comparisons. The survival of mice was analyzed with Prism GraphPad software. Isobologram analysis was performed using the CalcuSyn software. The significance of the *P* value is $*P < .05$, $**P < .01$, $***P < .001$, or $****P < .0001$, whenever indicated.

Results

CDK7 inhibition disrupts the CDK-RB-E2F axis in MM cells

After confirming the expression of the CDK-activating kinase complex members (CDK7, cyclin H, and MAT1) in primary MM cells and MM cell lines (supplemental Figure 1A-B), we investigated its function and activity in MM. Impairment of CDK7 expression and activity (via YKL-5-124) causes decreased MM cell proliferation, with significantly lesser sensitivity in phytohemagglutinin-activated normal donor peripheral blood mononuclear cells and nontransformed human cell lines (Figure 1A). These data were confirmed by CRISPR-Cas9 based genetic modulation and CDK7 rapid protein degradation using the degradation tag (dTAG) system (Figure 1B; supplemental Figure 1C). To evaluate on-target effect of CDK7 inhibition in MM cells we performed global phosphoproteomics after treatment with YKL-5-124, detecting a significant decreased phosphorylation within the T-loops of cell cycle CDKs (CDK1, CDK2, and CDK4/6) and their substrates (Figure 1C). These data were confirmed in several myeloma cell lines by western blot analysis, in which we also observed a decreased phosphorylation on Ser5 of the C-terminal domain of RNA polymerase II (Figure 1D-E; supplemental Figure 1D) after CDK7 inhibition.

Cell cycle analysis further showed that YKL-5-124 induced a significant accumulation of cells in G1 phase with a corresponding loss of cells in S phase (Figure 2A). Concomitant with the cell cycle arrest, we observed a potent reduction in phosphorylation of the retinoblastoma (Rb) protein after CDK7 inhibition (Figure 2B; supplemental Figure 2A). Because hypophosphorylated Rb acts as a repressor of the E2F transcriptional pathway, we evaluated the effects of CDK7 inhibition on E2F activity. We treated H929 MM cells harboring an E2F transcriptional activity reporter with YKL-5-124 and observed significant loss of reporter signal (Figure 2C).[12] Importantly, CDK7 inhibition caused depletion of chromatin bound E2F1 as assessed by EMSA (Figure 2D; supplemental Figure 2B), with its consequent displacement from the promoter regions of a set of direct target genes (Figure 2E). Moreover, we observed a positive correlation between expression of established myeloma E2F target genes (16) and expression of CDK7 in RNA-sequencing (RNA-seq) data of CD138$^+$ MM cells from 409 newly diagnosed patients (Figure 2F; supplemental Figure 2C). This association was also found in plasma cells derived from normal donors ($R = 0.55$), suggesting that CDK7 drives E2F activity in both normal as well as malignant conditions. However, we and others have shown that E2F activity is heightened in MM, especially in the relapse setting. Indeed, using a cohort of paired samples from patients at diagnosis and relapse (Determination study),[13] we confirmed increased E2F score in

Downloaded from http://ashpublications.net/blood/article-pdf/141/23/2841/2055728/blood_bld-2022-018885-main.pdf by guest on 06 May 2024

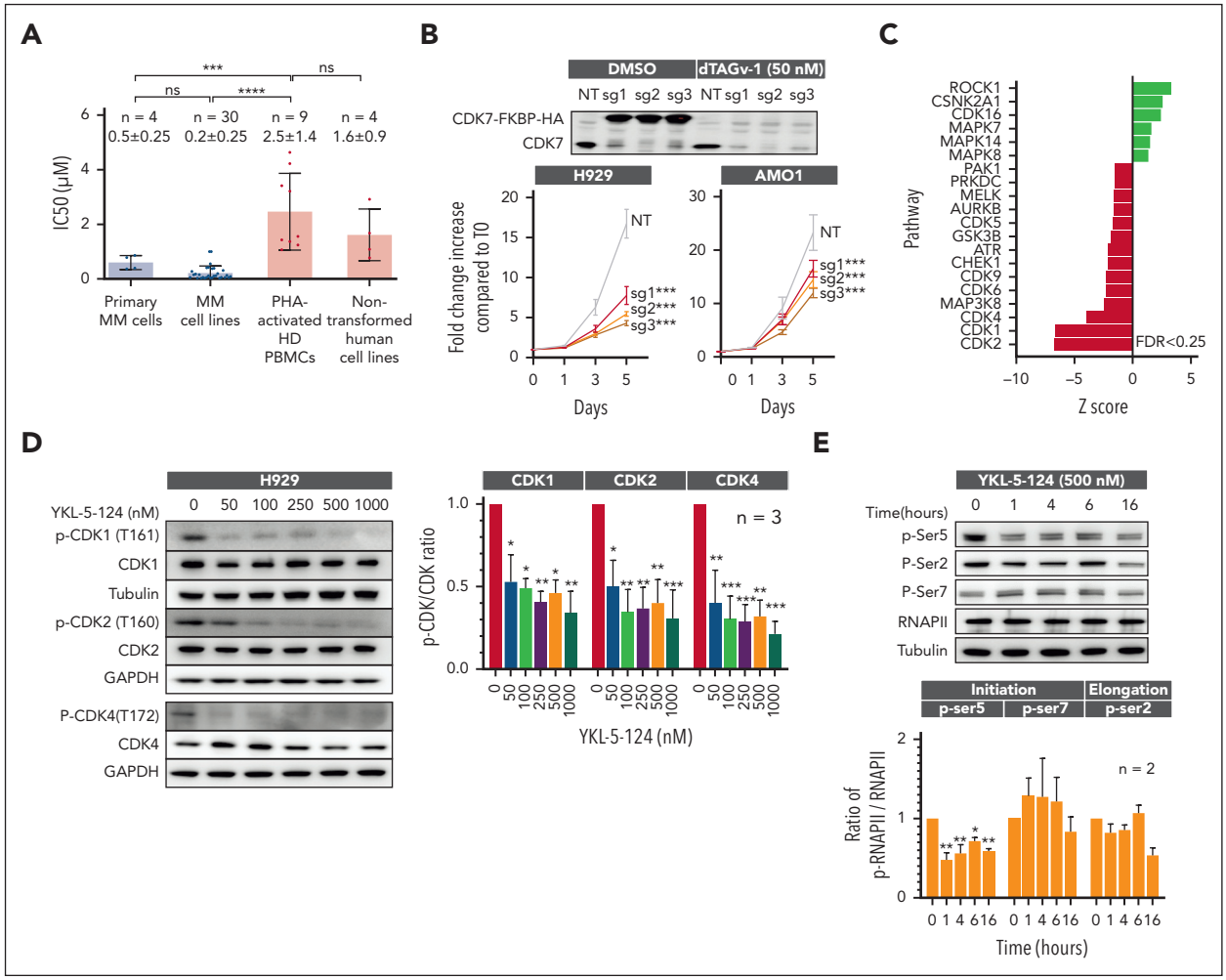

Figure 1. MM cells are selectively sensitive to CDK7 inhibition. (A) Primary cells from patients newly diagnosed with MM (n = 4), MM cell lines (n = 30), PHA-activated PBMCs (n = 9), and nontransformed human cell lines (GMO5756, IMR90, HEEpiC, and HS-5 cell lines) were treated with different concentrations of YKL-5-124 for 48 hours and assessed for cell viability using CellTiter-Glo (CTG). IC_{50} analysis was performed with GraphPad software. Data are shown as the mean value ± SD; ***$P < .001$. (B) H929 and AMO1 cells were engineered with a dTAG epitope (dTAG-$CDK7^{WT}$). Cell viability was measured in H929 dTAG-$CDK7^{WT}$ and AMO1 dTAG-$CDK7^{WT}$ cells after treatment with $dTAG^{V}$-1 by CTG and represented as fold change increase compared with time of seeding (T0). (C) Control and YKL-5-124–treated MM cells were subjected to global quantitative TMT-based proteomic and phosphoproteomic analyses. KSEA for prediction of kinase activity was applied to identify activated (green bars) and inhibited kinases (red bar) in the YKL-5-124–treated group compared with control cells. (D) Whole-cell lysates from H929 cells treated with several concentrations of YKL-5-124 for 24 hours were subjected to western blot (WB) analysis and probed with indicated antibodies, with GAPDH or tubulin as a loading control (left). The ratio of phosphorylated/total forms of indicated CDKs was analyzed with Image J software and represented as fold change from untreated cells. Mean values ± SD in 3 MM cell lines is shown in the graph (right). (E) Whole-cell lysates from H929 cells treated with several concentrations of YKL-5-124 for different times (1, 4, 6, and 16 hours) were subjected to WB analysis and probed with selected antibodies (upper). The ratio of phosphorylated/total RNA polymerase II was analyzed with Image J software and represented as fold change from untreated cells. Mean values ± SD in 3 MM cell lines is shown in the graph (lower). IC_{50}, 50% inhibitory; KSEA, kinase-substrate enrichment analysis; PBMCs, peripheral blood mononuclear cells; PHA, phytohemagglutinin; SD, standard deviation; TMT, tandem mass tag; WT, wild type.

relapsed patients (supplemental Figure 2D), which correlated significantly with CDK7 expression (R = 0.77; supplemental Figure 2E). These data confirm that CDK7 is a driver of E2F activity, and that E2F is hyperactivated in MM.

Importantly, ectopic expression in MM cells of the T121 fragment of the SV40 large T antigen inactivating the 3 members of the Rb family[14] restored E2F1 chromatin binding in cells treated with YKL-5-124 (Figure 2G; supplemental Figure 2F), confirming that CDK7 is an important hub in the CDK-Rb-E2F pathway via its ability to alleviate Rb-mediated repression of E2F.

Therefore, we tested whether Rb inactivation would alleviate the proliferative defects caused by CDK7 inhibition. Rb inactivation in cells expressing the T121 vector rescued the S phase arrest caused by YKL-5-124 (Figure 2H) but only partially overcame its induction of MM cell death (Figure 2I-J), suggesting that loss of RB1 only partially affects the sensitivity to CDK7 inhibition. These conclusions were strengthened by results from a genome-wide CRISPR–CRISPR-associated protein 9 (Cas9) knockout screen in the MM1S cell line treated with YKL-5-124 or vehicle, in which single guide RNAs targeting RB1 were indeed enriched (P = .001) but a modest effect (logFC = 0.2) was detected (supplemental Figure 2G). Altogether, these data suggest that the sensitivity to CDK7 inhibition is only partially dependent of functional RB1 and that CDK7 impacts other pathways critical for MM cell growth.

Downloaded from http://ashpublications.net/blood/article-pdf/141/23/2841/2055728/blood_bld-2022-018885-main.pdf by guest on 06 May 2024

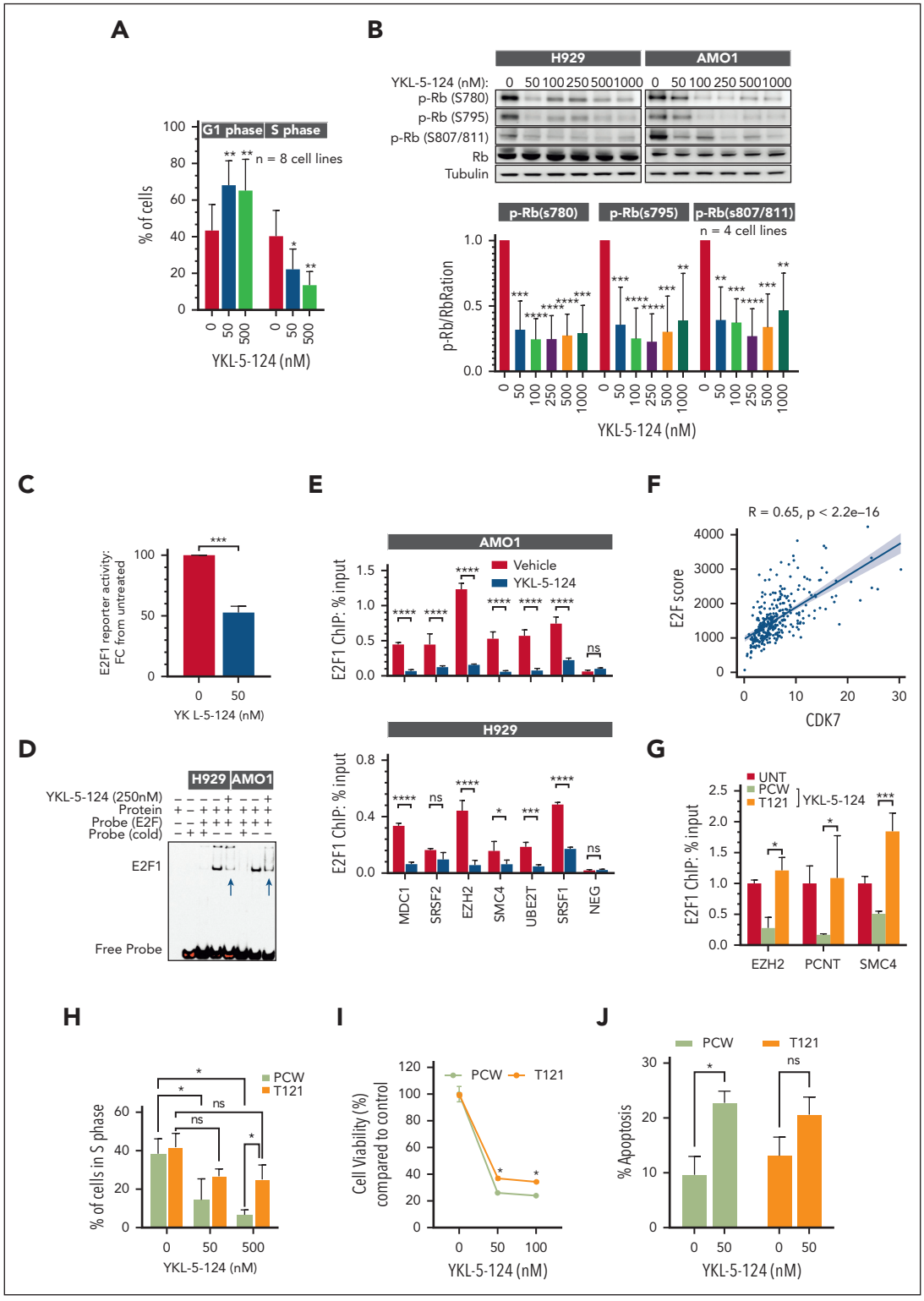

Figure 2. Impairment of T-loop phosphorylation by CDK7 inhibition causes cell cycle arrest and Rb activation in MM cells. (A) MM cell lines (n = 8) were treated with the indicated concentrations of YKL-5-124 for 24 hours. Cell cycle was evaluated by propidium iodide staining followed by flow cytometric analysis and analyzed with ModFit LT 5.0 software. (B) Whole-cell lysates from H929 and AMO1 cells treated with the indicated concentrations of YKL-5-124 for 24 hours were subjected to WB analysis and probed with antibodies against Rb and p-Rb, and GAPDH as a loading control. The ratio of phosphorylated/total forms of indicated Rb was analyzed with Image J software and represented as fold change from untreated cells. Mean values ± SD in 4 MM cell lines is shown in the graph. (C) H929 cells stably expressing E2F1 luciferase reporter were treated with 50 nM YKI-5-124 for 24 hours. E2F1 activity was assessed using the Promega luciferase reporter assay system, and fold change of E2F1 activity compared with untreated cells is displayed (mean ± SD). ***$P < .001$. (D) H929 and AMO1 cells were treated with 250 nM YKL-5-124 for 24 hours, and the nuclear extract was analyzed by EMSA. The shifted probe caused by E2F1 binding is indicated by the band labeled E2F1. (E) H929 and AMO1 cells were treated with 500 nM YKL-5-124 for 24 hours and chromatin immunoprecipitated using E2F1 or control mouse IgG antibodies. The crosslinked DNA was subjected to quantitative polymerase chain reaction using primers specific for a representative set of E2F1 target genes. Data are represented as the percentage of input. (F) E2F score was calculated by using E2F1 genes identified previously.[11] After

Downloaded from http://ashpublications.net/blood/article-pdf/141/23/2841/2055728/blood_bld-2022-018885-main.pdf by guest on 06 May 2024

CDK7 inhibition leads to selective transcriptional changes in cellular functions critical for MM cell survival

To further investigate the mechanisms of CDK7-mediated cell growth, we used global transcriptional profiling and unbiased gene set enrichment analysis after treating MM cell lines with YKL-5-124. At concentrations comparable with the 50% inhibitory values, YKL-5-124 treatment caused only a modest global reduction in per-cell messenger RNA (mRNA) levels, as seen using cell count spike-in normalized RNA-seq (supplemental Figure 3A), and produced selective and significant changes in a finite number of genes. These data are in contrast to prior studies that examined CDK7 function using less selective inhibitors, which showed a broad collapse of both normal and oncogenic transcription, probably because of a cumulative effect on multiple, independent transcription programs.[5,8,15,16] Across 6290 curated genes (MSigDB, C2), a highly concordant gene expression response between the cell lines was observed (Figure 3A). We confirmed that selective perturbation of CDK7 activity counteracts the molecular hallmarks of dysregulated cell cycle control at the G1/S checkpoint and downregulates E2F gene expression programs in MM cells by activating the dominant E2F repressor Rb (Figure 3A-B; supplemental Figure 3B). Along with the E2F signature, there was a significant downregulation of canonical MYC transcriptional programs and MYC-associated biological modules (eg, glycolysis and mTOR), whereas gene expression programs associated to other transcription factors with relevance to myeloma biology were not enriched (Figure 3A-B; supplemental Figure 3C). We also found these programs to be positively correlated with CDK7 gene expression in patient-derived tumor cell RNA-seq data (normalized enrichment score >2.0; false discovery rate <0.05). Total proteomic analysis in cells treated with YKL-5-124 confirmed a significant correlation between protein and mRNA level changes (supplemental Figure 3D-E).

Although E2F itself is an important upstream regulator of *MYC* transcription,[17] we explored whether CDK7 had a more direct role in regulating MYC levels or activity. In previous studies, transcriptional CDK inhibitors, such as THZ1 (CDK7/12/13) or those targeting CDK9, potently downregulated the transcription of MYC via targeting its upstream enhancer and super-enhancer elements and exploiting its high transcriptional rate and short mRNA half-life.[7] We confirmed that CDK7 affects MYC abundance and found that its inhibition caused a significant decrease in MYC protein levels within 2 hours of YKL-5-124 treatment or CDK7 protein degradation (Figure 3C, supplemental Figure 3G). In contrast, the levels of 2 other short– half-life proteins (MCL1 and cyclin D1) were unchanged (supplemental Figure 3F). Conversely, overexpression of CDK7 led to significant upregulation in MYC protein levels (supplemental Figure 3G). MYC protein reduction was independent of Rb activation (supplemental Figure 3H) and not a secondary consequence of perturbed cell cycle progression (data not shown).

To gain insights into the mechanisms by which CDK7 regulates MYC levels, we have performed a time course analysis after addition of cycloheximide (CHX) to block de novo protein synthesis (cycloheximide chase assay), which revealed a decrease in MYC half-life, suggestive of an additive effect with YKL-5-124 (supplemental Figure 4A). In addition, we inhibited the 2 major protein degradation pathways in eukaryotic cells, the ubiquitin-proteasome system (with MG132) and autophagy (with chloroquine). We indeed found that treatment with proteasome inhibitor MG132 but not chloroquine (data not shown) partially rescued the MYC protein degradation observed upon CDK7 inhibition (supplemental Figure 4B-C). Moreover, we observed a slight increase in MYC Thr58 phosphorylation after short exposure to YKL-5-124 (data not shown). However, although YKL-5-124 in Raji cells carrying a T58 MYC mutation failed to decrease MYC protein levels (supplemental Figure 4D), expression of a MYC Thr58 phosphorylation–dead mutant, T58A, in H929 MM cells only partially rescued the CDK7i-induced loss of MYC (supplemental Figure 4E). Most likely the observed MYC loss upon CDK7 perturbation is the result of impact on multiple regulatory mechanisms responsible for MYC steady-state cellular levels including proteasome-dependent MYC-degradation.

Regulation of cellular metabolism is one of the mechanisms used by MYC to affect tumor cells.[18-20] Our transcriptomic analysis revealed that CDK7 activity is required for the expression of many components of the glycolytic cascade (Figure 3D). Whole proteomic analysis in MM cells confirmed HK2 among the most downregulated proteins after YKL-5-124 treatment or CDK7 protein degradation (Figure 3E; supplemental Figure 5A). These data were reproduced in additional MM cell lines by western blot analysis (Figure 3F). In these cells, lactate dehydrogenase A (LDHA) was also decreased (supplemental Figure 5B) whereas pyruvate dehydrogenase and glucose transporter protein type 1 showed no effect (supplemental Figure 5C).

HK2 and LDHA have been described as transcriptional targets of MYC.[21-23] We confirmed the binding of MYC to the DNA promoter region of HK2 and LDHA (Figure 3G), which was diminished in the presence of YKL-5-124 (Figure 3H); and that MYC modulation causes changes in the expression (supplemental Figure 5H), suggesting that HK2 and LDHA are transcriptional targets of MYC in myeloma cells as well.

Blocking CDK7 stalls the proliferation of MM by reducing aerobic glycolysis

Both *HK2* and *LDHA* have been implicated in MM pathobiology and response to therapy.[24,25] Analysis of CRISPR essentiality screen data in the Cancer Dependency Map (Avana library

Figure 2 (continued) RNA-seq normalization, we converted expression values for each gene to z scores, with a mean of 0 and SD of 1. After scaling the expression, we calculated the total score as the sum of scaled scores from all the genes. A Pearson correlation coefficient was calculated between E2F score and CDK7 expression. (G) AMO1 cells expressing control vector (PCW) or T121 were treated with doxycycline for 24 hours, followed by YKL-5-124 (500 nM) for 6 hours, and then chromatin immunoprecipitated using E2F1 or control mouse IgG antibodies. The crosslinked DNA was subjected to quantitative polymerase chain reaction using primers specific for a representative set of E2F1 target genes. Data are represented as the percentage of input. (H) AMO1 cells expressing either PCW or T121 plasmid were treated with doxycycline for 24 hours, followed by YKL-5-124 for 24 hours. The cell cycle was evaluated by propidium iodide staining followed by flow cytometric analysis. (I-J) MM cells expressing either control or T121 plasmid were treated with doxycycline for 24 hours followed by YKL-5-124 treatment for 48 hours. Cell viability was measured by CTG assay (I) and apoptosis by annexin V^+ staining (J). Data represent the mean of 4 independent experiments. IgG, immunoglobulin G; SD, standard deviation.

Downloaded from http://ashpublications.net/blood/article-pdf/141/23/2841/2055728/blood_bld-2022-018885-main.pdf by guest on 06 May 2024

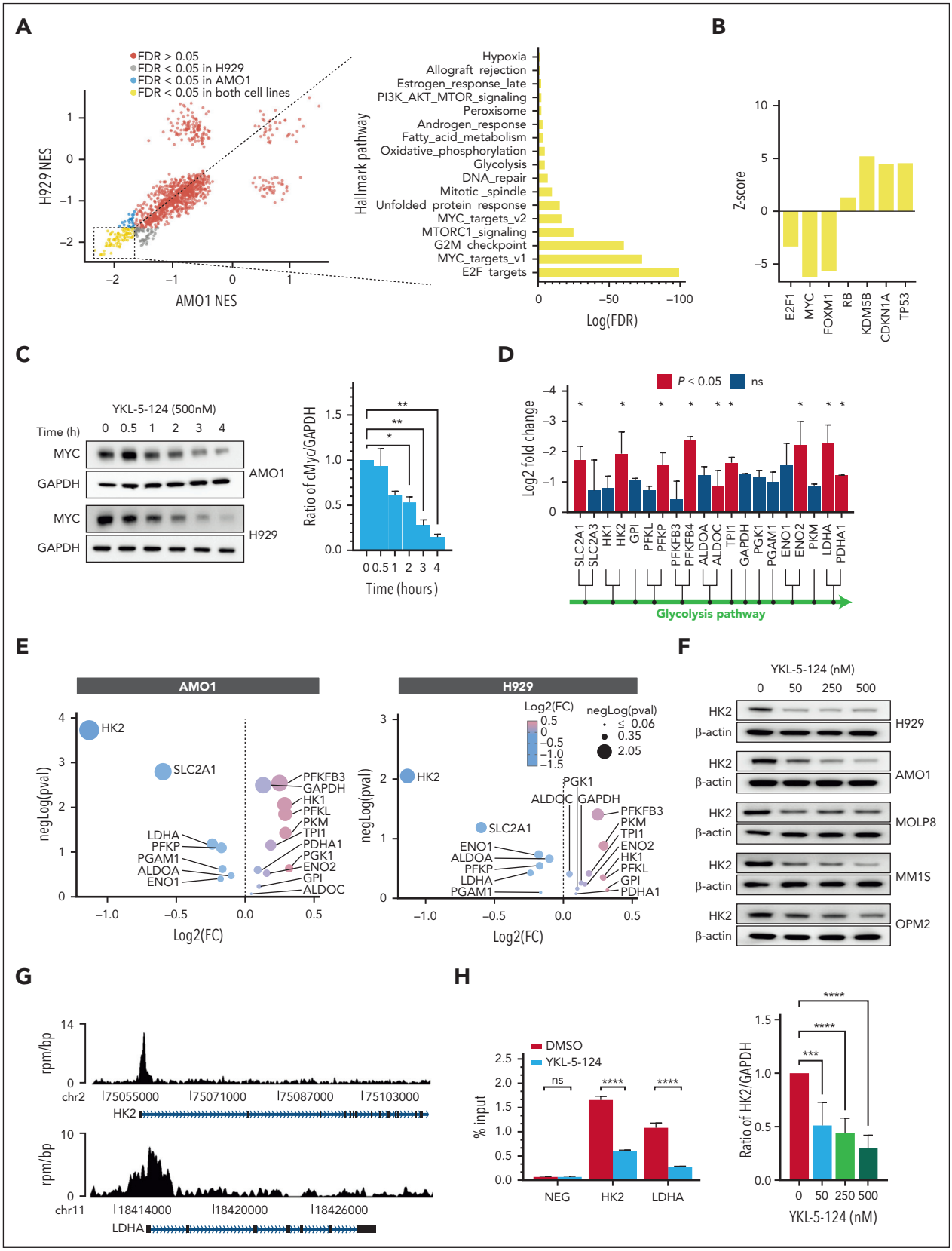

Figure 3. YKL-5-124 treatment disrupts oncogenic gene expression programs in MM. (A) Scatter plot visualizing gene set enrichment analysis normalized enrichment score comparisons between H929 and AMO1 cells treated with DMSO or YKL-5-124 (100 nM) for 24 hours. The bar graph shows NES for the top 18 gene signatures in both cell lines after treatment with YKL-5-124. (B) Biological upstream regulators associated with CDK7 inhibition were identified using ingenuity pathway analysis (IPA). (C) Whole-cell lysates from AMO1 and H929 cells treated with YKL-5-124 for 0.5 to 4 hours were subjected to WB analysis and probed with MYC antibody, with GAPDH as a loading control. The ratio of MYC/GAPDH was analyzed with Image J software and represented as fold change from untreated cells. Mean values ± SD in 2 MM cell lines is shown in the graph.

Downloaded from http://ashpublications.net/blood/article-pdf/141/23/2841/2055728/blood_bld-2022-018885-main.pdf by guest on 06 May 2024

public 18Q448), across >400 cancer cell lines, further confirmed that myeloma has among the strongest genetic dependencies on HK2 (Figure 4A). The dependency of myeloma on HK2 was confirmed in an independent CRISPR–Cas9 KO screen in 17 MM cell lines[26] (supplemental Figure 5D). These data support an important role for HK2 in myeloma and provide the rationale to focus on the potential role of CDK7 in regulating glucose metabolism in MM cells.

A glycolysis stress test with Seahorse XFe96 analyzer using extracellular acidification rate as a measure of glycolytic activity showed that CDK7-inhibited MM cells have significant defects in glycolysis and glycolytic capacity (Figure 4B-C; supplemental Figure 5E-F). Although enforced expression of MYC increases the glycolytic rates in MM cells (supplemental Figure 5G), silencing of MYC in MM cells resulted in a further reduction (supplemental Figure 5H-I). The defect in glycolysis was also observed in vivo in which short exposure to YKL-5-124 blocked glucose consumption in MM cell xenografts as assessed by [^{18}F]-fluorodeoxyglucose positron emission tomography imaging, with no significant impact on tumor volume (Figure 4D). The effect of CDK7 inhibition on glycolysis was however independent from Rb activation (supplemental Figure 5J-K). HIF-1a is also implicated as a key regulator of the glycolytic phenotype in cancer.[27,28] Our experiments were conducted at atmospheric oxygen concentrations, and HIF1α mRNA and protein levels were undetectable in MM cells and were not modulated by CDK7i (data not shown), providing evidence of an HIF1α-independent mechanism.

Given that cancer cells catabolize glucose to lactate in a process enabled by LDHA, we explored the effect of CDK7 inhibition on LDHA enzymatic activity and lactate production by MM cells. A sharp time-dependent increase in extracellular lactate release was observed in MM cells over time, and ablation of CDK7 decreased both LDHA enzymatic activity and lactate release (Figure 4E-F), with no effect on expression of the lactic acid transporters (MCT1 and MCT4) responsible for the export of lactate into the extracellular space (data not shown).

To evaluate the effect of cellular glycolysis rates on MM cell proliferation during CDK7 inhibition, we ectopically overexpressed HK2 in MM cells and observed a relatively higher 50% inhibitory for YKL-5-124 compared with control cells (Figure 4G). Moreover, combining YKL-5-124 with glycolysis inhibitor 2DG[29] did not cause a further inhibition of MM cell proliferation, suggesting that they have similar mechanisms of action (supplemental Figure 5L). However, overexpression of CDK7 rendered MM cells more vulnerable to 2DG treatment (data not shown). Finally, CDK7 inhibition suppressed the ability of MM cells to grow in glucose. In contrast, culturing cells in galactose-containing medium, which reduces glycolytic flux and forces cells to depend on mitochondrial oxidative phosphorylation for energy production (Leloir pathway), significantly reduces sensitivity to CDK7 inhibition (Figure 4H). These data suggest a role for CDK7 in supporting growth in highly glycolytic cellular systems, and that the effect of CDK7 inhibition is partially mediated by the modulation of MYC-dependent glycolysis.

Accumulating evidence implicates altered energy metabolism in acquired drug resistance of myeloma cells,[25,30] and elevated aerobic glycolysis was observed in bortezomib, dexamethasone, and melphalan resistance settings.[31,32] We indeed observed that overall CDK7 inhibition can enhance the therapeutic efficacy of proteasome inhibitors (bortezomib and carfilzomib), the immunomodulatory drug lenalidomide, and the DNA-damaging agent melphalan, even in resistant cell models and in cells ectopically overexpressing HK2 (Figure 4I; supplemental Figure 6A-C). Together, these data suggest that pharmacological inhibition of CDK7 may be an effective strategy for targeting and circumventing drug resistance in MM and other tumor types with enhanced glycolytic rates.

CDK7 is a therapeutic vulnerability in MM that can be targeted by YKL-5-124

Because YKL-5-124 is a specific CDK7 inhibitor with high translational potential, we lastly assessed its efficacy and mechanism of action in therapeutically relevant myeloma models and contexts.

Because MM cells rely on their surrounding microenvironment for survival, we first confirmed the effect of CDK7 inhibition on CD138$^+$ primary MM cells from patients with myeloma in the presence of their bone marrow milieu. Treatment with YKL-5-124 caused decreased cellular proliferation in CD138$^+$ myeloma cells without any impact on the normal CD138$^-$ population (Figure 5A). These data were confirmed in a panel of MM cell lines cultured in the presence of bone marrow stromal cells (BMSCs) from patients with MM (supplemental Figure 7A). Moreover, an increase in apoptotic cell death was observed in primary MM cells upon inhibition of CDK7 (Figure 5B).

We then evaluated the impact of CDK7 inhibition via YKL-5-124 on tumor growth in vivo in several murine models of MM. H929 MM cells were injected subcutaneously into mice and treated with vehicle or YKL-5-124 when tumors reached 100 mm^3 (early treatment model) or ~500 mm^3 (late treatment model) (Figure 5C). Compared with vehicle injection, intraperitoneal injection of YKL-5-124 for 2 weeks in both early and late treatment models almost completely eradicated the tumor growth without evident toxicity (Figure 5D; supplemental Figure 7B). Identical results were obtained in mice injected

Figure 3 (continued) (D) The diagram depicts the intermediates of glycolysis, and the enzymes regulated by CDK7 (red bars). Mean of log2-fold change for H929 and AMO1 cells after treatment with YKL-5-124 are shown (*P < .05). (E) Bubble plot showing the differentially expressed proteins involved in the glycolytic pathway after treatment with YKL-5-124 for 24 hours. The x-axis displays the log2 (fold change), and the y-axis represents the negative log of the adjusted P value. (F) A panel of cells treated with YKL-5-124 for 24 hours was subjected to western blot analysis and probed with antibodies against HK2 and β-actin as a loading control (upper panel). The ratio of HK2/actin was analyzed with Image J software and represented as fold change from untreated cells (lower panel). Mean values ± SD in 5 MM cell lines are shown in the graph. (G) ChIP-seq tracks showing MYC signal on individual loci for LDHA and HK2. The x-axis shows genomic coordinates with gene model depicted below. The y-axis shows signal in units of rpm/bp. (H) MM1S cells were treated with YKL-5-124 for 6 hours and subjected to ChIP with a MYC or IgG antibody. HK2, LDHA, and a negative control region were amplified by polymerase chain reaction. Data are shown as mean ± SD of triplicates and represented as the percentage of input. bp, base pair; ChIP, chromatin immunoprecipitation; CHIP, clonal hematopoiesis of indeterminate potential; DMSO, dimethyl sulfoxide; FDR, false discovery rate; IgG, immunoglobulin G; NES, normalized enrichment score; rpm, units of reads per million; SD, standard deviation.

Downloaded from http://ashpublications.net/blood/article-pdf/141/23/2841/2055728/blood_bld-2022-018885-main.pdf by guest on 06 May 2024

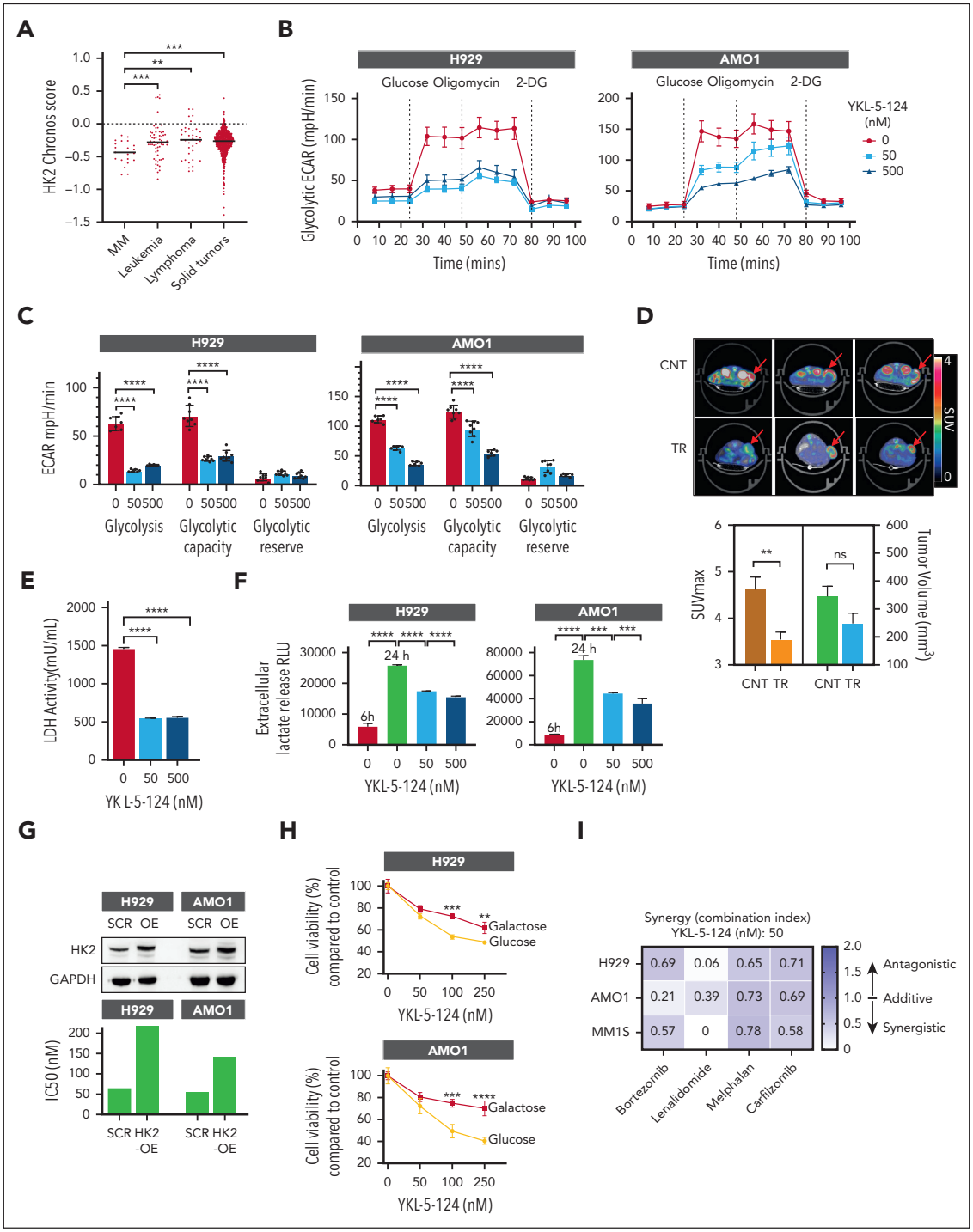

Figure 4. MYC-dependent aerobic glycolysis is impaired in CDK7-inhibited MM cells. (A) DepMap CRISPR screen (Avana library 18Q4) dependency data indicating that MM cell lines are among the most sensitive to HK2 depletion based on cell line rank. Mean of chronos scores for each disease type are shown in the graph. (B-C) H929 and AMO1 cells were treated with DMSO or YKL-5-124 and analyzed with a glycolysis stress assay on a Seahorse XFe96 extracellular flux analyzer. (B-C) ECAR was detected at baseline, after injection of glucose, oligomycin, and 2-deoxy-D-glucos e (2-DG). Basal glycolytic rate and spare glycolytic capacity were analyzed by overall ECAR in control and YKL-5-124–treated groups at different concentrations of YKL-5-124. (D) Representative ^{18}F-FDG PET-computed tomography images (upper panel) and quantification (lower panel) of H929 cell xenografts in mice after treatment (10 mg/kg YKL-5-124 or vehicle, for 3 days). Bar graphs represent the SUV maximum and corresponding TV for mice. (E) LDH activity was measured in cell lysate from AMO1 cells treated with YKL-5-124 for 24 hours. (F) Culture supernatant (5 μL) from both untreated cells after 6 and 24 hours of culture, and 24 hour–treated cells was used to measure lactate secretion using Lactate-Glo assay. (G) H929 and AMO1 cells were transduced with empty vector or HK2-overexpression vector and subjected to western blot analysis or treated with YKL-5-124 for 72 hours for cell killing assessment. IC_{50} values are shown in the graph. (H) H929 and AMO1 cells were cultured in glucose or galactose (10 mM) media for a week and treated with DMSO or increasing concentrations of YKL-5-124. Cellular viability was determined by CTG assay. (I) Three MM cell lines (H929, AMO1, and MM1S) were cultured in the presence of different concentrations of YKL-5-124 with or without bortezomib (2.5 nM), lenalidomide (5 μM), melphalan (2.5 μM), or carfilzomib (1 nM), and cell survival was assessed by CTG. Data are presented as CI values evaluated using the Calcusyn software. CI, combination index; DMSO, dimethyl sulfoxide; ECAR, extracellular acidification rate; IC_{50}, 50% inhibitory; PET, positron emission tomography; SUV, standardized uptake value; TV, tumor volume.

Downloaded from http://ashpublications.net/blood/article-pdf/141/23/2841/2055728/blood_bld-2022-018885-main.pdf by guest on 06 May 2024

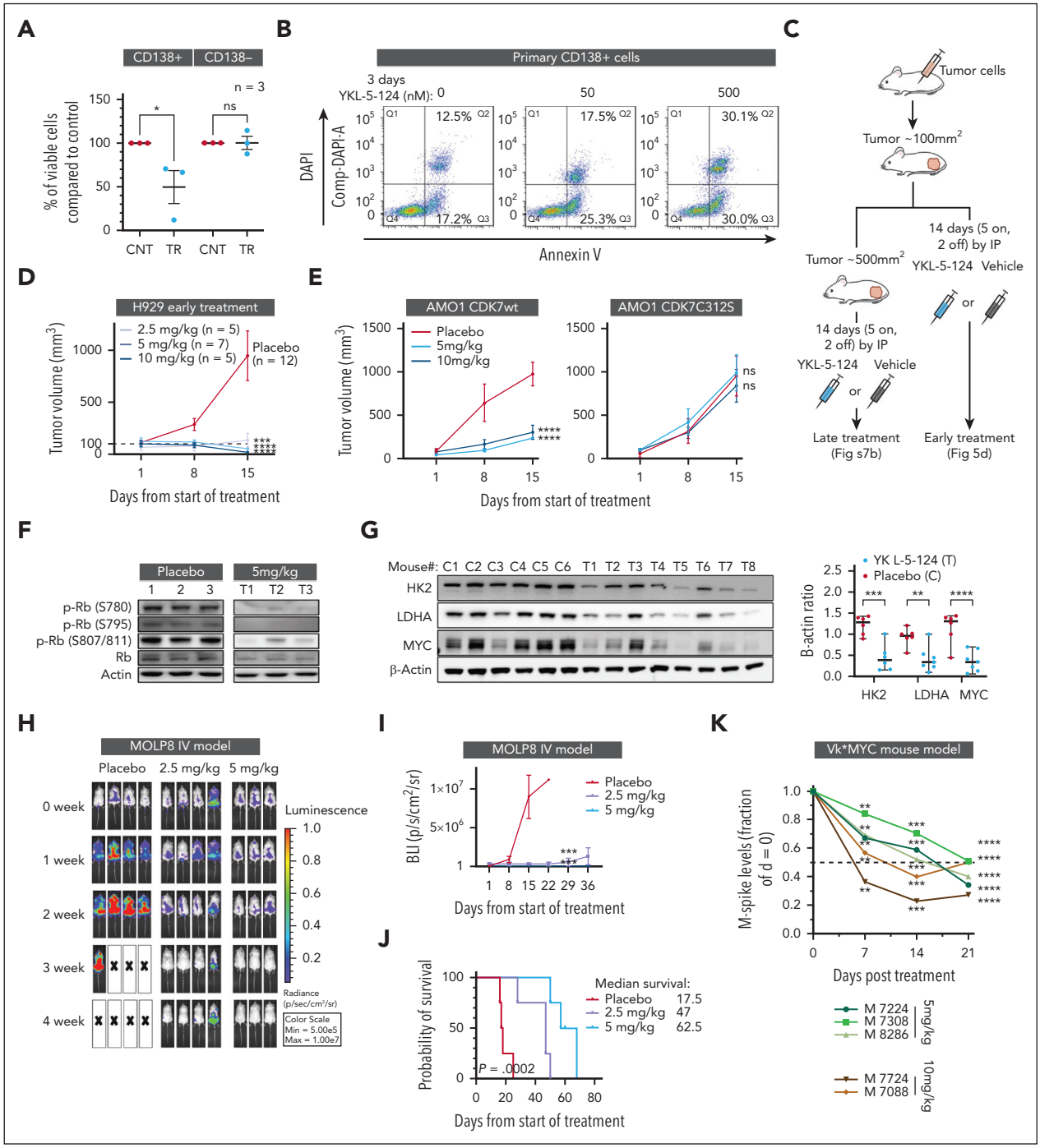

Figure 5. CDK7 inhibition reduces myeloma burden and enhances survival in vivo mouse models of MM. (A) BMMNC from 3 patients with relapsed MM were treated with 500 nM YKL-5-124 or DMSO for 24 hours. Cell viability in the CD138$^+$ and CD138$^-$ cell populations was evaluated by flow cytometry analysis. (B) Primary CD138$^+$ cells were cultured in the absence or presence of YKL-5-124 for 3 days, and apoptotic cell death was assessed by flow cytometric analysis. Percentages of annexin V$^+$/DAPI$^-$ (early apoptosis) and annexin V$^+$/DAPI$^+$ (late apoptosis) cells are shown in the graphs. (C) A schematic diagram for the subcutaneous SCID model. (D) In the early treatment model, mice injected with H929 cells were randomized and treated with either YKL-5-124 or vehicle at first detection of tumor (tumor volume ~100 mm^3). Mice received 3 different doses of YKL-5-124 for 5 consecutive days per week for 2 weeks. Tumor volume was measured in 2 perpendicular dimensions by caliper once every week. Baseline values were not significantly different among groups. (E) Sublethally irradiated SCID mice were injected subcutaneously with AMO1 cells expressing CDK7^{WT} (left) or CDK7^{C312S} (right). Mice were randomized to a 5 or 10 mg/kg group, for 5 consecutive days per week for 2 weeks. Tumor volume was evaluated by caliper measurement. *P* values indicate significant difference between groups. ***$P < .001$. (F) Western blot analysis was performed in cell lysates from tumors excised from representative mice and blotted with Rb and p-Rb antibodies. (G) Western blot analysis was performed in cell lysates from tumors excised from representative mice and blotted with indicated antibodies. Images were analyzed with Image J software and signals normalized to loading control. (H-J) NSG mice were orthotopically xenografted after intravenous injection with Molp8-luc cells. Upon detection of MM lesions (~2 weeks after tumor cell injection), mice were randomly assigned to receive YKL-5-124 (2.5 or 5 mg/kg, intraperitoneal, 5 days per week, for 4 weeks) or vehicle control. Whole-body bioluminescence images (BLI) (H) and measurements (mean ± SEM) (I) are shown. Survival was evaluated from the first day of treatment until death. Survival curves (Kaplan-Meier) were analyzed using GraphPad analysis software (log-rank test, $P = .0002$) (J). (K) Monoclonal, tumor-derived, immunoglobulin (M-protein) levels were evaluated in MM-bearing Vk*MYC mice before and after YKL-5-124 treatment (5 and 10 mg/kg) and normalized to time 0. BMMNC, bone marrow mononuclear cells; DMSO, dimethyl sulfoxide; NSG, NOD/SCID-γ; SCID, severe combined immunodeficiency.

Downloaded from http://ashpublications.net/blood/article-pdf/141/23/2841/2055728/blood_bld-2022-018885-main.pdf by guest on 06 May 2024

with MM1S MM cell line and treated with a low dose of YKL-5-124 (1 mg/kg) (supplemental Figure 7C).

To confirm the specificity of CDK7 inhibition in vitro and in vivo, we engineered 2 MM cell lines to express $CDK7^{C312S}$, which harbors a mutation of the reactive cysteine to a less nucleophilic serine (C312S), thus preventing YKL-5-124 from covalently binding. In these mutant cells, YKL-5-124 failed to decrease cell proliferation and CDK7-driven activities both in vitro (supplemental Figure 7D) and in vivo (Figure 5E). Moreover, evaluation of tumors retrieved from mice after treatment revealed significant reduction in Rb phosphorylation (Figure 5F) as well as HK2, c-MYC, and LDHA levels (Figure 5G) compared with control mice.

Next, we tested the efficacy of CDK7 inhibition via YKL-5-124 in 2 disseminated (IV) myeloma models. In a MOLP8-luc dissemination model, YKL-5-124 treatment significantly reduced MM burden, as measured with a serial assessment of whole-body bioluminescence (Figure 5H-I), leading to increased overall survival (Figure 5J). These results were reproduced in an H929-luc disseminated model, in which a significant decrease in tumor burden was observed despite the short treatment cycle because of the extremely fast growth of this tumor (supplemental Figure 7E-F).

Finally, the effect of CDK7 inhibition was explored in a transgenic mouse model that activates MYC in germinal center B cells (Vk*MYC).[33] In this model, a low dose of YKL-5-124 caused a decline in the amount of monotypic serum immunoglobulins, indicative of a positive response (Figure 5K). Altogether, these data support CDK7 as a functionally relevant and pharmacologically accessible target for MM with emerging evidence of a good therapeutic index.

Discussion

MM is a plasma cells malignancy with recurrent genetic alterations of cell cycle, growth, and metabolic regulators. Although the transcription factors in these deregulated pathways (eg, MYC or E2F) are considered conventionally undruggable, there is active ongoing clinical investigation into whether targeting druggable cofactors, such as CDK7, can selectively block oncogenic transcription factor activity.[15,34]

We have shown previously that altered control of E2F-dependent transcription represents an additional oncogenic transcriptional regulatory axis in MM that is distinct from the enhancer and BET-bromodomain regulated transcriptional axis associated with plasma cell identity.[11] In the present study, we show that E2F activity is heightened in MM, especially in the relapse setting, and is significantly correlated with expression of CDK7. E2F is tightly controlled by the activity of cell cycle CDKs, which phosphorylate and release the E2F-complexing repressor protein Rb. Here, we show that CDK7 inhibition restrains E2F activity by increasing the functionality of Rb, and may therefore circumvent compensatory mechanisms by other cell cycle–associated kinases more effectively, as observed for US Food and Drug Administration–approved CDK4/6 inhibitors, yielding therapeutic advantages. However, in our study Rb inactivation did not cause a complete rescue of the antiproliferative properties of CDK7 inhibition in MM cells, demonstrating that CDK7 controls additional pathways relevant to myeloma cell growth.

Indeed, our data suggest that in addition to E2F, CDK7 inhibition impedes MYC dysregulation in MM by regulating its cellular levels. The proto-oncogene MYC plays a critical role in various cellular functions including the metabolic reprogramming of cancer cells. MM is 1 of several cancers that exhibits abnormal glucose metabolism evident from increased positron emission tomography positivity, and this increased dependence on glycolysis stems from MYC deregulation. Altered glucose metabolism with the rewiring of metabolic pathways has been reported in myeloma with impact on drug sensitivity.[25,30,35,36] In this study we show that CDK7 inhibition causes a perturbation of the expression of genes involved in the glycolytic cascade in a MYC-dependent manner, ultimately reducing the rate of glycolysis and lactate production in MM cells. HK2 catalyze the first committed step in glucose metabolism and is expressed at high level in MM cells but only at a limited level in normal adult tissues.[24,37] The strong genetic dependency on HK2 observed in MM cells could render MM cells more vulnerable to the disruption of glucose metabolism, explaining the striking activity of CDK7 inhibitor YKL-5-124 in MM cells compared with their normal counterparts.

The regulation of MYC-dependent glucose metabolism by CDK7 in MM cells builds on recent work providing evidence of a co-regulation between cell cycle progression and cellular metabolism,[38,39,40] suggesting CDKs as targetable cellular nodes at the intersection between these 2 fundamental processes.

Moreover, although simultaneous inhibition of multiple transcriptional CDKs may increase the risk of toxicity in normal tissues, this study shows that chemical inhibition of CDK7 catalytic function via YKL-5-124 causes gene-specific, rather than global, repression of transcription and is generally tolerated by normal cells while eliciting a strong therapeutic response in MM cells.

In the clinical setting, selective inhibition of CDK7 might be most useful in combination with other standard-of-care agents used in clinical management of MM, and indeed we detected a strong synergism with conventional antimyeloma agents even in resistant settings or in cells overexpressing HK2. These data confirm that CDK7 inhibition is a valuable novel therapeutic intervention, alone and in combination in MM. High lactic acid and hypoxic microenvironments have been shown to contribute to immune escape, leading to resistance to cancer immunotherapy. The observation that CDK7 inhibition reduces the levels of lactate produced by MM cells and released in the extracellular space provide the rationale for future evaluation of the impact of CDK7 inhibition on the myeloma immune microenvironment and immune cell functions, which could lead to future combination with immunotherapies.

In conclusion, we herein report a specific vulnerability in MM cells upon disruption of the CDK7-driven molecular programs, supporting a model in which cell cycle, transcriptional, and metabolic deregulation are counteracted by inhibition of CDK7 activity, leading to cell cycle arrest and subsequent apoptosis in MM. With the observed encouraging preclinical evidence of a therapeutic window, CDK7 may therefore represent a new

Downloaded from http://ashpublications.net/blood/article-pdf/141/23/2841/2055728/blood_bld-2022-018885-main.pdf by guest on 06 May 2024

molecular vulnerability with unique mechanism of actions to be exploited with the specific inhibitor YKL-5-124.

Acknowledgments

The authors thank Christina Usher for comments on the manuscript; and Ryan Young for sharing the CRISPR screen data. The authors are grateful for the technical support of Quang-De Nguyen and Louise M. Clark of the Lurie Family Imaging Center, Dana-Farber Cancer Institute.

This study was supported by National Institutes of Health (NIH)/National Cancer Institute (NCI) P01 grant (CA155258-10) to M.F., K.C.A., and N.C.M.; a Department of Veterans Affairs I01 grant (BX001584-09) to N.C.M.; NIH/NCI R01 grant (CA207237-05), and a Paula and Rodger Riney Foundation grant to K.C.A.; NIH/NCI SPORE grant (P50-CA100707-18) to N.C.M. and K.C.A.; National Natural Science Foundation of China (81870163) and Major Basic Research Project of the Natural Science Foundation of the Jiangsu Higher Education Institutions (19KJA560001) to Y.Y.; LLS Special Fellow grant and ASH Scholar Award to E.M. M.C. was supported by the NCI (U54-CA224018 and RO1-CA234181).

Authorship

Contribution: M.F., C.Y.L., and N.C.M. designed and conducted the study and wrote the manuscript; Y.Y. performed the in vitro and in vivo experiments, and analyzed the data; J.F.N. and W.D.P. performed gene expression analysis; M.C. performed the Vk*MYC animal experiment; J.F.N., E.M., S.D., J.E.M., Z.C., Y.X., and C.E. helped with the in vitro and in vivo experiments; M.S. analyzed patient RNA-seq analysis data; N.S.G., B.N., and N.K. provided the reagents for pharmacological and genetic studies; and R.A.Y., N.K., C.M., and K.C.A. provided critical evaluation of experimental data and manuscript.

Conflict-of-interest disclosure: N.K. is now an employee of Kymera Therapeutics, Inc. N.S.G. is a founder, science advisory board member, and equity holder in Syros, C4, Allorion, Jengu, B2S, Inception, EoCys, Larkspur (board member), and Soltego (board member). The Gray laboratory receives, or has received, research funding from Novartis, Takeda, Astellas, Taiho, Janssen, Kinogen, Arbella, Deerfield, and Sanofi. N.S.G. and N.K. are named inventors on patent claiming YKL-5-124. K.C.A. has received consulting fees from Bristol-Myers Squibb (BMS), Celgene, Gilead, Janssen, Precision Biosciences, Sanofi-Aventis, Takeda, and Tolero; and serves on the board of directors of, and has stock options in, Oncopep. N.C.M. is a consultant for BMS, Janssen, Oncopep, Amgen, Karyopharm, Legened, AbbVie, Takeda, and GSK; and serves on the board of directors of, and stock options in, Oncopep. C.Y.L. is an executive and shareholder of Kronos Bio; has licensed intellectual property to Syros Pharmaceuticals; and is a shareholder and adviser of Ovibio, which is involved in the commercialization of YKL-5-124. R.A.Y. is a founder and equity holder in Syros Pharmaceuticals. B.N. is an inventor on patent applications related to the dTAG system (WO/2017/024318, WO/2017/024319, WO/2018/148440, WO/2018/148443, and WO/2020/146250). M.C. has received royalties for the Vk*MYCDLox technology. C.M. serves on the scientific advisory board of Adicet Bio; and discloses consultant/honoraria from Genentech, Fate Therapeutics, Ionis Pharmaceuticals, FIMECS, Secura Bio, and Oncopeptides; and discloses research funding from Janssen/Johnson & Johnson, EMD Serono, Arch Oncology, Karyopharm, Sanofi, Nurix, BMS, H3 Biomedicine/Eisai, Springworks, Abcuro, and Novartis. The remaining authors declare no competing financial interests.

ORCID profiles: W.D.P., 0000-0002-4069-4954; E.M., 0000-0002-8850-0442; J.E.M., 0000-0003-4479-9822; Z.C., 0000-0003-4807-2532; Y.X., 0000-0002-6167-3319; C.E., 0000-0001-8358-8345; B.N., 0000-0002-6738-4200; M.C., 0000-0002-4024-8225; N.S.G., 0000-0001-5354-7403; R.A.Y., 0000-0001-8855-8647; C.Y.L., 0000-0002-9155-090X.

Correspondence: Mariateresa Fulciniti, Medical Oncology, Dana-Farber Cancer Institute, 450 Brookline Ave, Boston, MA 02215; email: mariateresa_fulciniti@dfci.harvard.edu; and Nikhil C. Munshi, Dana-Farber Cancer Institute, 450 Brookline Ave, Boston, MA 02215; email: nikhil_munshi@dfci.harvard.edu.

Footnotes

Submitted 27 October 2022; accepted 18 February 2023; prepublished online on *Blood* First Edition 6 March 2023. https://doi.org/10.1182/blood.2022018885.

RNA-seq data are available at GEO under accession number GSE172445.

Data are available on request from corresponding author Mariateresa Fulciniti (mariateresa_fulciniti@dfci.harvard.edu).

The online version of this article contains a data supplement.

There is a *Blood* Commentary on this article in this issue.

The publication costs of this article were defrayed in part by page charge payment. Therefore, and solely to indicate this fact, this article is hereby marked "advertisement" in accordance with 18 USC section 1734.

REFERENCES

1. Deshpande A, Sicinski P, Hinds PW. Cyclins and cdks in development and cancer: a perspective. *Oncogene*. 2005;24(17):2909-2915.
2. Tiedemann RE, Mao X, Shi CX, et al. Identification of kinetin riboside as a repressor of CCND1 and CCND2 with preclinical antimyeloma activity. *J Clin Invest*. 2008;118(5):1750-1764.
3. Ramanathan Y, Rajpara SM, Reza SM, et al. Three RNA polymerase II carboxyl-terminal domain kinases display distinct substrate preferences. *J Biol Chem*. 2001;276(14):10913-10920.
4. Glover-Cutter K, Larochelle S, Erickson B, et al. TFIIH-associated Cdk7 kinase functions in phosphorylation of C-terminal domain Ser7 residues, promoter-proximal pausing, and termination by RNA polymerase II. *Mol Cell Biol*. 2009;29(20):5455-5464.
5. Wang Y, Zhang T, Kwiatkowski N, et al. CDK7-dependent transcriptional addiction in triple-negative breast cancer. *Cell*. 2015;163(1):174-186.
6. Zhang H, Christensen CL, Dries R, et al. CDK7 inhibition potentiates genome instability triggering anti-tumor immunity in small cell lung cancer. *Cancer Cell*. 2020;37(1):37-54.e9.
7. Chipumuro E, Marco E, Christensen CL, et al. CDK7 inhibition suppresses super-enhancer-linked oncogenic transcription in MYCN-driven cancer. *Cell*. 2014;159(5):1126-1139.
8. Zhang Y, Zhou L, Bandyopadhyay D, et al. The covalent CDK7 inhibitor THZ1 potently induces apoptosis in multiple myeloma cells in vitro and in vivo. *Clin Cancer Res*. 2019;25(20):6195-6205.
9. Nabet B, Roberts JM, Buckley DL, et al. The dTAG system for immediate and target-specific protein degradation. *Nat Chem Biol*. 2018;14(5):431-441.
10. Olson CM, Liang Y, Leggett A, et al. Development of a selective CDK7 covalent inhibitor reveals predominant cell-cycle phenotype. *Cell Chem Biol*. 2019;26(6):792-803.e10.
11. Fulciniti M, Lin CY, Samur MK, et al. Non-overlapping control of transcriptome by promoter- and super-enhancer-associated dependencies in multiple myeloma. *Cell Rep*. 2018;25(13):3693-3705.e6.
12. Teh JLF, Cheng PF, Purwin TJ, et al. In vivo E2F reporting reveals efficacious schedules of MEK1/2-CDK4/6 targeting and mTOR-S6 resistance mechanisms. *Cancer Discov*. 2018;8(5):568-581.
13. Richardson PG, Jacobus SJ, Weller EA, et al. Triplet therapy, transplantation, and

Downloaded from http://ashpublications.net/blood/article-pdf/141/23/2841/2055728/blood_bld-2022-018885-main.pdf by guest on 06 May 2024

maintenance until progression in myeloma. *N Engl J Med*. 2022;387(2):132-147.

14. Santamaria D, Barriere C, Cerqueira A, et al. Cdk1 is sufficient to drive the mammalian cell cycle. *Nature*. 2007;448(7155):811-815.
15. Christensen CL, Kwiatkowski N, Abraham BJ, et al. Targeting transcriptional addictions in small cell lung cancer with a covalent CDK7 inhibitor. *Cancer Cell*. 2014;26(6):909-922.
16. Jia Y, Zhou J, Tan TK, et al. Myeloma-specific superenhancers affect genes of biological and clinical relevance in myeloma. *Blood Cancer J*. 2021;11(2):32.
17. Oswald F, Lovec H, Moroy T, Lipp M. E2F-dependent regulation of human MYC: trans-activation by cyclins D1 and A overrides tumour suppressor protein functions. *Oncogene*. 1994;9(7):2029-2036.
18. Dang CV. MYC, metabolism, cell growth, and tumorigenesis. *Cold Spring Harb Perspect Med*. 2013;3(8):a014217.
19. Morrish F, Hockenbery D. MYC and mitochondrial biogenesis. *Cold Spring Harb Perspect Med*. 2014;4(5):a014225.
20. van Riggelen J, Yetil A, Felsher DW. MYC as a regulator of ribosome biogenesis and protein synthesis. *Nat Rev Cancer*. 2010;10(4):301-309.
21. Kim JW, Zeller KI, Wang Y, et al. Evaluation of myc E-box phylogenetic footprints in glycolytic genes by chromatin immunoprecipitation assays. *Mol Cell Biol*. 2004;24(13):5923-5936.
22. Dang CV, Le A, Gao P. MYC-induced cancer cell energy metabolism and therapeutic opportunities. *Clin Cancer Res*. 2009;15(21):6479-6483.
23. Marinkovic D, Marinkovic T, Kokai E, Barth T, Moller P, Wirth T. Identification of novel Myc target genes with a potential role in lymphomagenesis. *Nucleic Acids Res*. 2004;32(18):5368-5378.
24. Ikeda S, Abe F, Matsuda Y, Kitadate A, Takahashi N, Tagawa H. Hypoxia-inducible hexokinase-2 enhances anti-apoptotic function via activating autophagy in multiple myeloma. *Cancer Sci*. 2020;111(11):4088-4101.
25. Maiso P, Huynh D, Moschetta M, et al. Metabolic signature identifies novel targets for drug resistance in multiple myeloma. *Cancer Res*. 2015;75(10):2071-2082.
26. Yang Y, Bolomsky A, Oellerich T, et al. Oncogenic RAS commandeers amino acid sensing machinery to aberrantly activate mTORC1 in multiple myeloma. *Nat Commun*. 2022;13(1):5469.
27. Kaelin WG Jr, Ratcliffe PJ. Oxygen sensing by metazoans: the central role of the HIF hydroxylase pathway. *Mol Cell*. 2008;30(4):393-402.
28. Lum JJ, Bui T, Gruber M, et al. The transcription factor HIF-1alpha plays a critical role in the growth factor-dependent regulation of both aerobic and anaerobic glycolysis. *Genes Dev*. 2007;21(9):1037-1049.
29. Pelicano H, Martin DS, Xu RH, Huang P. Glycolysis inhibition for anticancer treatment. *Oncogene*. 2006;25(34):4633-4646.
30. Zaal EA, Wu W, Jansen G, Zweegman S, Cloos J, Berkers CR. Bortezomib resistance in multiple myeloma is associated with increased serine synthesis. *Cancer Metab*. 2017;5:7.
31. Gu Z, Xia J, Xu H, Frech I, Tricot G, Zhan F. NEK2 promotes aerobic glycolysis in multiple myeloma through regulating splicing of pyruvate kinase. *J Hematol Oncol*. 2017;10(1):17.
32. Zub KA, de Sousa MML, Sarno A, et al. Modulation of cell metabolic pathways and oxidative stress signaling contribute to acquired melphalan resistance in multiple myeloma cells. *PLoS One*. 2015;10(3):e0119857.
33. Chesi M, Robbiani DF, Sebag M, et al. AID-dependent activation of a MYC transgene induces multiple myeloma in a conditional mouse model of post-germinal center malignancies. *Cancer Cell*. 2008;13(2):167-180.
34. Kwiatkowski N, Zhang T, Rahl PB, et al. Targeting transcription regulation in cancer with a covalent CDK7 inhibitor. *Nature*. 2014;511(7511):616-620.
35. Bloedjes TA, de Wilde G, Guikema JEJ. Metabolic effects of recurrent genetic aberrations in multiple myeloma. *Cancers*. 2021;13(3):396.
36. Wu S, Kuang H, Ke J, Pi M, Yang DH. Metabolic reprogramming induces immune cell dysfunction in the tumor microenvironment of multiple myeloma. *Front Oncol*. 2020;10:591342.
37. Caillot M, Bourgeais J, Dakik H, et al. Cyclin D1 targets hexokinase 2 to control aerobic glycolysis in myeloma cells. *Oncogenesis*. 2020;9(7):68.
38. Galbraith MD, Andrysik Z, Pandey A, et al. CDK8 kinase activity promotes glycolysis. *Cell Rep*. 2017;21(6):1495-1506.
39. Wang H, Nicolay BN, Chick JM, et al. The metabolic function of cyclin D3-CDK6 kinase in cancer cell survival. *Nature*. 2017;546(7658):426-430.
40. Ghezzi C, Wong A, Chen BY, et al. A high-throughput screen identifies that CDK7 activates glucose consumption in lung cancer cells. *Nat Commun*. 2019;10:5444.

Licensed under Creative Commons Attribution-NonCommercial-NoDerivatives 4.0 International (CC BY-NC-ND 4.0), permitting only noncommercial, nonderivative use with attribution.

Downloaded from http://ashpublications.net/blood/article-pdf/141/23/2841/2055728/blood_bld-2022-018885-main.pdf by guest on 06 May 2024